ANTIMICROBIAL AGENTS AND CHEMOTHERAPY, Mar. 2005, p. 963–972 Vol. 49, No. 3
0066-4804/05/$08.00+0 doi:10.1128/AAC.49.3.963–972.2005

Small-Molecule Inhibitors of the Budded-to-Hyphal-Form Transition in the Pathogenic Yeast *Candida albicans*

Kurt A. Toenjes,[1] Suzanne M. Munsee,[1] Ashraf S. Ibrahim,[2] Rachel Jeffrey,[1] John E. Edwards, Jr.,[2] and Douglas I. Johnson[1]*

Department of Microbiology and Molecular Genetics and Markey Center for Molecular Genetics, University of Vermont, Burlington, Vermont,[1] and Division of Infectious Diseases, St. John's Cardiovascular Research Center, Harbor-UCLA Research and Education Institute, Torrance, California[2]

Received 5 August 2004/Returned for modification 20 August 2004/Accepted 22 October 2004

The pathogenic yeast *Candida albicans* can exist in multiple morphological states, including budded, pseudohyphal, and true hyphal forms. The ability to convert between the budded and hyphal forms, termed the budded-to-hyphal-form transition, is important for virulence and is regulated by multiple environmental and cellular signals. To identify inhibitors of this morphological transition, a microplate-based morphological assay was developed. With this assay, the known actin-inhibiting drugs latrunculin-A and jasplakinolide were shown to inhibit the transition in a dose-dependent and reversible manner. Five novel small molecules that reversibly inhibited the transition and hyphal elongation without affecting budded growth were identified. These molecules inhibited hyphal growth induced by Spider, Lee's, M199 pH 8, and 10% serum-containing media, with two molecules having a synergistic effect. The molecules also differentially affected the hyphal form-specific gene expression of *HWP1* and endocytosis without disrupting the actin cytoskeleton or septin organization. Structural derivatives of one of the molecules were more effective inhibiters than the original molecule, while other derivatives had decreased efficacies. Several of the small molecules were able to reduce *C. albicans*-dependent damage to endothelial cells by inhibiting the budded-to-hyphal-form transition. These studies substantiated the effectiveness of the morphological assay and identified several novel molecules that, by virtue of their ability to inhibit the budded-to-hyphal-form transition, may be exploited as starting points for effective antifungal therapeutics in the future.

The polymorphic yeast *Candida albicans* is the most common causative agent of systemic human fungal infections, and *Candida* species are the fourth most common cause of nosocomial septicemia (13). This commensal organism is a major opportunistic pathogen of immunocompromised and immunosuppressed individuals, including those with AIDS and those who are undergoing chemotherapy or tissue transplants (36). *C. albicans* virulence can be attributed to its ability to survive and thrive in multiple organs, the mucosa, and the bloodstream of the host and to virulence factors that aid in adherence to and invasion of epithelial and endothelial cell types (8, 26, 28). Insights into the virulence mechanisms of *C. albicans* are likely to lead to the development of new prophylactic and therapeutic strategies, a point that is especially critical because of the significant increases in resistance to current antifungal therapeutics within the patient population (reviewed in references 30 and 50).

C. albicans cells exist in different morphological states, including a budded or yeast-like form and pseudohyphal and true hyphal filamentous forms (Fig. 1). The ability to switch between morphological states, referred to herein as the budded-to-hyphal-form transition, is critical for systemic infections, a premise that has been reinforced by the reduced virulence of various *C. albicans* mutants that are defective in hypha formation (12, 16, 19–21, 33, 40, 52). The budded-to-hyphal-form transition occurs in response to a variety of external signals, including elevated temperature or pH, nitrogen and/or carbon starvation, the presence of host macrophages, and growth in serum or other chemicals such as *N*-acetylglucosamine (6).

Multiple intracellular signaling pathways respond to these different growth and environmental signals to induce or repress hyphal development (7, 23). The Cst20p-Hst7p-Cek1p mitogen-activated protein kinase pathway, which is homologous to the Ste20p-Ste7p-Kss1p pathway in *Saccharomyces cerevisiae*, signals downstream from the Cdc42p GTPase to the Cph1p transcription factor to induce hyphal form-specific genes (12, 17, 19, 24). The Efg1p transcription factor functions downstream of the Ras GTPase and Tpk2p, the catalytic component of protein kinase A, to integrate a cyclic AMP signal into hyphal development (14, 25, 41, 43). Recent data also indicate that Efg1p functions downstream of the Cdc42p GTPase (46). Activation of these different signaling pathways ultimately leads to rearrangements of the actin- and tubulin-based cytoskeleton (1, 53) and expression of hyphal form-specific genes, including *HWP1*, which is regulated by the Efg1p pathway but not the Cph1p pathway (5, 7, 38). The molecular mechanisms that underlie these different signaling pathways and their potential cross talk are unclear.

C. albicans is a constitutively diploid organism that lacks a meiotic sexual cycle and has limited mating ability, making standard genetic approaches for the isolation of recessive, loss-of-function mutants not currently possible. Therefore, alternative strategies for the identification of components participat-

* Corresponding author. Mailing address: Department of Microbiology and Molecular Genetics, 202 Stafford Hall, 95 Carrigan Dr., University of Vermont, Burlington, VT 05405. Phone: (802) 656-8203. Fax: (802) 656-8749. E-mail: Douglas.Johnson@uvm.edu.

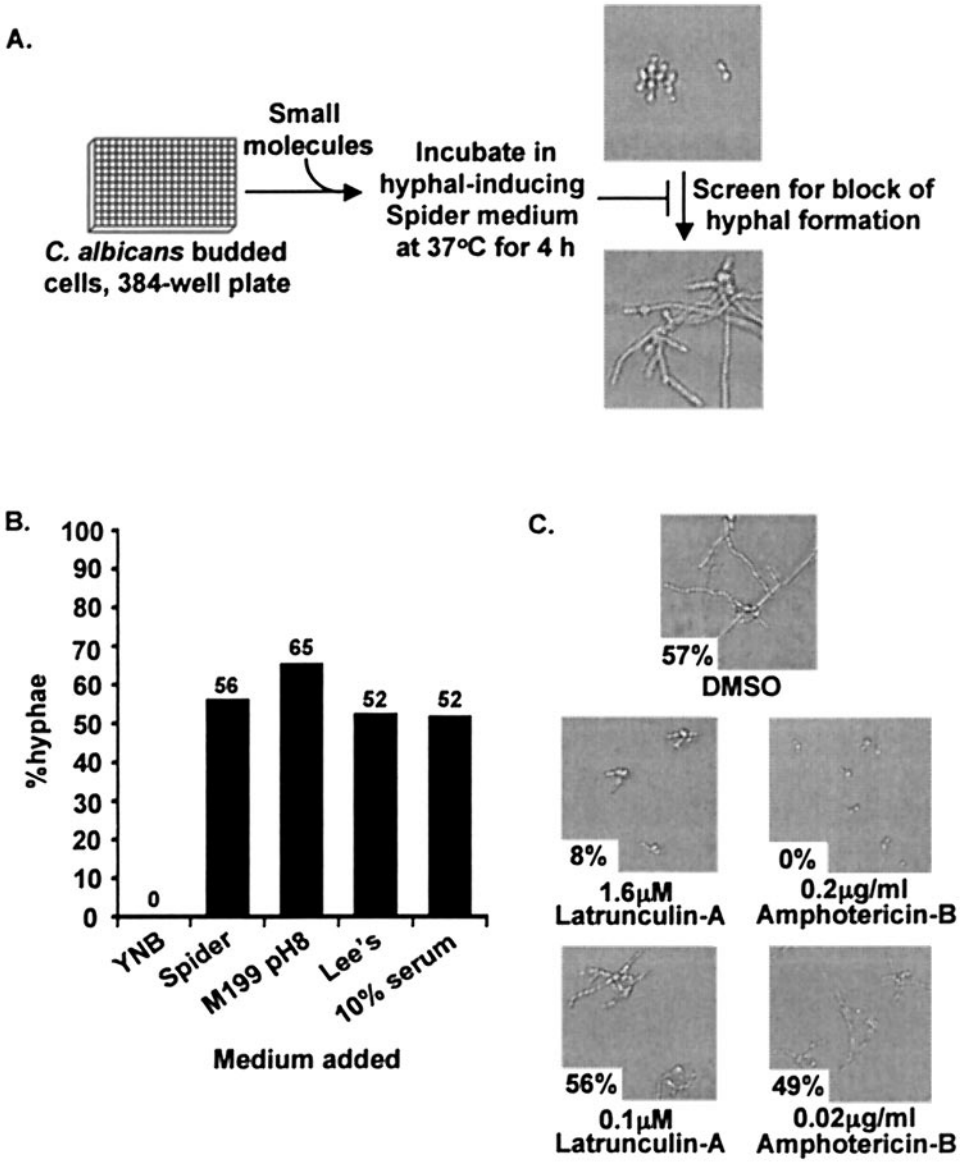

FIG. 1. Budded-to-hyphal-form transition and its inhibition by latrunculin A. (A) Microplate-based morphological assay. (B) SC5314 cells grown in YNB medium were transferred to 384-well optical microplates containing either Spider medium, YPD plus 10% fetal calf serum, Lee's medium, or M199 pH 8 tissue culture medium and incubated at 37°C for 4 h. The percentage of hyphae observed is shown above each bar. (C) SC5314 cells grown in YNB medium were transferred to 384-well optical micoplates containing Spider medium and either latrunculin A (1.6 or 0.1 μM) or amphotericin B (0.2 or 0.02 μg/ml) and incubated at 37°C for 4 h. The percentage of hyphae observed is shown in the lower left of each photomicrograph.

ing in the budded-to-hyphal-form transition are needed. One such approach is to screen large, diverse sets of small organic molecules for inhibitory effects on the budded-to-hyphal-form transition. This type of "forward genetic" approach has been successful in studying a wide variety of biological processes (reviewed in references 11, 31, and 47), including the recent identification of a small molecule that inhibits the growth of *C. albicans* (45).

For this study, a small-molecule screen was developed, and a proof-of-concept study with known actin-inhibitory molecules verified that the assay was robust and reproducible. Five novel small molecules that inhibited the budded-to-hyphal-form transition without affecting normal budded growth were identified, and their action was shown to be dose dependent and reversible. Analysis of structural derivatives of one of these molecules identified two variants that were more effective as well as several less-effective variants. Two of the molecules were also able to inhibit *C. albicans*-induced endothelial cell injury, indicating that these molecules are likely to inhibit *C. albicans* virulence. This approach will significantly augment known genetic and biochemical strategies used to identify components that regulate the budded-to-hyphal-form transition and may facilitate the identification of potential antifungal therapeutic molecules and targets.

MATERIALS AND METHODS

Reagents, media, and strains. Enzymes, PCR kits, and other reagents were obtained from standard commercial sources and used as specified by the suppliers. Protocols for the growth and maintenance of bacterial strains (34) and *C. albicans* strains (39) were described previously. To induce hyphal growth, stationary-phase cultures were diluted into 5 ml of either YPD (1% yeast extract, 2% peptone, and 2% dextrose) plus 10% (vol/vol) fetal calf serum, Spider medium (24), Lee's medium (9, 22), or M199 pH 8 medium (Sigma-Aldrich, St. Louis, Mo.), as indicated, and grown in 50-ml flasks at 37°C with shaking at 250 rpm.

The following *Candida albicans* strains were used in this study: SC5314 (wild-type clinical isolate); BWP17 (*ura3*::λ*imm434*/*ura3*::λ*imm434 his1*::*hisG*/*his1*::*hisG arg4*::*hisG*/*arg4*::*hisG*; kindly provided by Aaron Mitchell, Columbia University (51); YAW2 (*pADH-CDC10-GFP ura3*::λ*imm434*/*ura3*::λ*imm434 his1*::*hisG*/*his1*::*hisG arg4*::*hisG*/*arg4*::*hisG*; kindly provided by James Konopka, Stony Brook University (49); CAI4 (*ura3*::λ*imm434*/*ura3*::λ*imm434* (4); and KTCa1 (*URA3-pHWP1-GFP ura3*::λ*imm434*/*ura3*::λ*imm434*; this study).

To create strain KTCa1, strain CAI4 was transformed (18) with plasmid pHWP1-GFP (42), kindly provided by Paula Sundstrom, Dartmouth University, that had been cleaved with the Cla1 endonuclease. Ura^+ transformants that had pHWP1-GFP stably integrated into the genome and that expressed green fluorescent protein (GFP) under the control of the *HWP1* promoter (HWP1 *pr*-GFP) were identified. Induction of HWP1 *pr*-GFP was observed by growth on Spider medium or YNB (0.67% yeast nitrogen base, 2% dextrose, and required amino acids) plus 10% fetal calf serum at 37°C.

Microplate-based morphological assay. The *C. albicans* SC5314 cells used in the growth assay were derived from a single colony grown on YPD plus uridine (80 mg/liter) solid medium and then inoculated into a 5-ml culture of YNB plus 2% glucose. After growth overnight at 30°C with shaking, the culture was diluted 1:25,000 into Spider medium, and 100 μl was placed into each well of a 384-well microplate (Falcon 353962). In the initial screen, small molecules (Chembridge Corp., San Diego, Calif.) dissolved in dimethyl sulfoxide were added to each well at 100 μM concentrations, and the plate was incubated at 37°C for 4 h. After 4 h, the cells in each well were fixed by adding electron microscopy-grade glutaric dialdehyde (Acros Organics/Fisher Scientific, Pittsburgh, Pa.) to a final concentration of 5% (vol/vol) for light microscopy or electron microscopy-grade formaldehyde (Ted Pella, Inc., Redding, Calif.) to a final concentration of 4% (vol/vol) for fluorescence microscopy.

Quantification of inhibition of the budded-to-hyphal-form transition was accomplished by counting the number of individual budded cells versus the number of hyphae in the population. More than 100 cells were counted for each well in duplicate, and all assays were repeated at least twice. Large-budded cells (i.e., buds were comparable in size to the mother cells) were counted as two cells, while small-budded cells (i.e., buds were smaller than the mother cells) were counted as one cell. This method, which was necessitated by the aggregation of budded cells that could not be resolved by sonication, resulted in an underrepresentation of the number of budded cells in the population. Individual hyphae were counted as one cell, although the hyphae usually consisted of multiple individual hyphal cells. This method, which was necessitated by the inability to quantify individual cells within hyphae, also resulted in an underrepresentation of the number of hyphal cells in the population. The percentage of hyphae reported is normalized to the percentage of hyphae formed when no molecule was added. The lowest effective concentration of inhibitory molecule (i.e., lowest concentration at which ≤10% hyphae were observed) was determined with serial dilutions of the individual molecules.

To test for cytotoxicity, a quantitative growth assay was performed. *C. albicans* cells were incubated with the molecules for 24 h at 37°C in Spider medium, at which time the wells were checked for turbidity and the cells were examined morphologically. The well contents were resuspended by pipetting, and 5 μl plus serial dilutions were incubated on YPD plus uridine plates at 37°C.

The reversibility assay was performed as described for the budded-to-hyphal morphological assay with the following modifications. After 4 h of incubation at 37°C, the medium was removed, and the cells were washed once with Spider medium, resuspended in 100 μl of Spider medium, and incubated for 8 h at 37°C before fixation. For the elongation assay, SC5314 cells were induced in Spider medium for 2 h at 37°C prior to the addition of the bioactive molecules, and hyphal elongation was assayed 4 h after the addition. For the synergy assay, two different molecules (100 μM) were added together, and the assay was performed as described above. All pairwise combinations of molecules were tested.

Fluorescent microscopy. For light microscopy, *C. albicans* cells in 384-well microplates with an optical plastic bottom (Falcon 353962) were routinely viewed on a Nikon TE300 microscope with differential interference/Hoffman optics and a 20X objective. Images of each well were obtained with a SpotRT monochrome camera driven by *In Vivo* software (QED Imaging, Pittsburgh, Pa.). For fluorescent microscopy, *C. albicans* cells in 384-well microplates with an optical-glass bottom (BD Falcon 357312) were viewed on a Nikon TE300 microscope with Nikon filter sets.

Induction of *HWP1* expression was determined with KTCa1 cells in the assay as described above with a GFP HYQ filter set and a 20X objective. To stain the vacuoles of SC5314 cells, the assay was carried out as above for 3 h, and then FM4-64 was added at 5 μg/ml and the plate was returned to 37°C for 30 min. Medium containing FM4-64 was then aspirated out of each well, and 100 μl of fresh medium was added. The plate was returned to 37°C, and the cells were viewed at 30, 60, 90, and 120 min with the Nikon TE300 microscope with the stage heated to 37°C, a G-1B filter set, and a 100X objective for wells containing budded cells or a 60X objective for wells containing hyphal cells.

To determine the localization of the septin proteins, YAW2 cells were used in the assay described above with a Nikon TE300 inverted microscope, a GFP HYQ filter set, and a 100X objective. Where indicated, cells from the same culture but different fields were assembled into collages with Adobe Photoshop 7.0.

Endothelial cell damage assay. The ability of small molecules to protect human umbilical vein endothelial cells (HUVECs) against damage by the SC5314 strain of *C. albicans* was determined with the chromium (^{51}Cr) release assay in 96-well tissue culture plates described previously (32). The ability of small molecules to induce ^{51}Cr release in the absence of added *C. albicans* cells (toxicity to endothelial cells) was also determined. Briefly, HUVECs grown in 96-well tissue culture plates containing detachable wells were incubated with $Na_2{}^{51}CrO_4$ (ICN, Irvine, Calif.) in M-199 medium (1 μCi per well) for 16 h. On the day of the experiment, the unincorporated ^{51}Cr was aspirated, and the wells were washed twice with warmed Hanks' balanced salt solution (Irvine Scientific). To determine the effect of small molecules on *C. albicans*-induced endothelial cell injury, HUVECs were infected with 4×10^4 blastospores of *C. albicans* (150 μl) in RPMI 1640 medium (Irvine Scientific) supplemented with glutamine in the presence or absence of various concentrations of these small molecules. Spontaneous ^{51}Cr release was determined by incubating HUVECs in RPMI 1640 medium supplemented with glutamine without *C. albicans*. To measure the toxicity of these small molecules, HUVECs were incubated with RPMI 1640 medium containing the desired concentration of the small molecules without the addition of *C. albicans.* After 3 h of incubation at 37°C in a 5% CO_2 incubator, 50% of the medium (75 μl) was aspirated from each well and transferred to glass tubes, and the cells were manually detached and placed into another set of tubes. The amount of ^{51}Cr in the aspirate and the detached well was determined by gamma counting.

The total amount of ^{51}Cr incorporated by HUVECs in each well equaled the sum of radioactive counts per minute of the aspirated medium plus the radioactive counts of the corresponding detached wells. After the data were corrected for variations in the amount of tracer incorporated in each well, the percentage of specific HUVEC release of ^{51}Cr (due to *C. albicans* or due to toxicity of the molecules) was calculated by the following formula: [(experimental release × 2) − (spontaneous release × 2)]/[total incorporation − (spontaneous release × 2)] × 100. When assessing the role of small molecules on *C. albicans*-induced injury, ^{51}Cr release due to molecule toxicity (no *C. albicans* infection) was subtracted from ^{51}Cr release due to *C. albicans* in the presence of the tested molecule. Each experimental condition was tested in triplicate with endothelial cells collected from different umbilical cords in three separate experiments. The small molecules were added to final concentrations of 40 or 100 μM.

RESULTS

Microplate-based assay allows detection of the budded-to-hyphal-form transition responding to different hypha-inducing media and known inhibitors. In the budded-to-hyphal growth assay, SC5314 cells were grown in YNB medium to maintain them in a budded state and then transferred to 384-well optical microplates containing Spider medium to induce the budded-to-hyphal-form transition and hyphal elongation (Fig. 1A). Microscopic examination indicated that *C. albicans* cells underwent the budded-to-hyphal-form transition and showed significant hyphal elongation within 4 h at 37°C in Spider medium (Fig. 1B). The budded-to-hyphal-form transition was also clearly observed in 384-well optical plates with other hypha-inducing media, including YPD plus 10% fetal

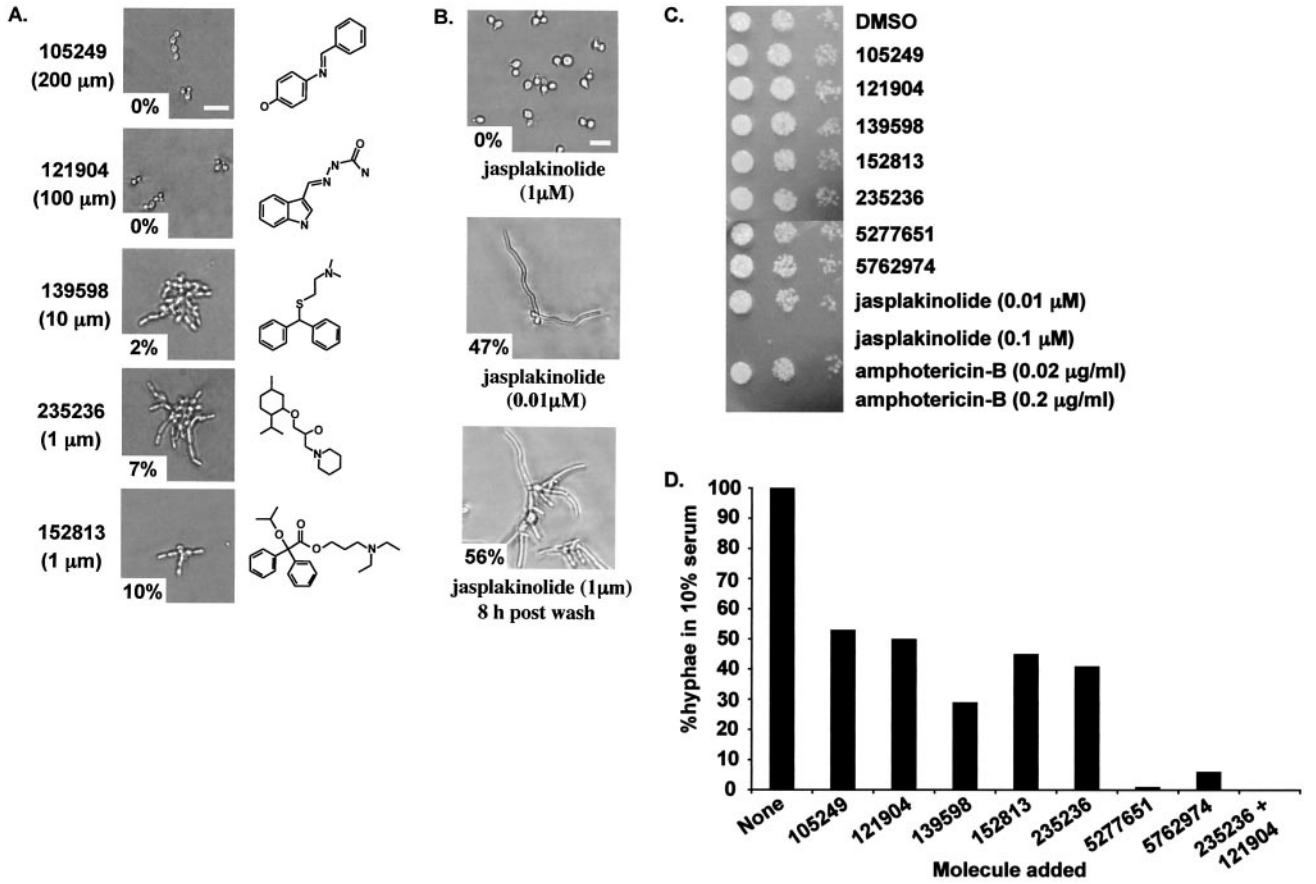

FIG. 2. New small molecules that inhibited the budded-to-hyphal-form transition. Morphological assays were performed as described for Fig. 1. (A) The indicated small molecules (Chembridge catalog number and chemical structure are shown) were initially added to cells at 100 μM concentrations. The concentrations shown are the minimal concentration tested that gave ≤10% hyphal growth at 37°C for 4 h. The percentage of hyphae observed is shown in the lower left of each photomicrograph. (B) The actin-stabilizing drug jasplakinolide (one of the original unknown molecules) was added at 1 and 0.01 μM concentrations, and cells were observed after 4 h at 37°C. The reversibility of drug action was shown by washing out the jasplakinolide and incubating the cells in Spider medium for 8 h at 37°C. (C) Cytotoxicity assay. The small molecules were added at a 200 μM concentration or as indicated for jasplakinolide and amphotericin B, and growth was assayed on YPD plus uridine plates at 37°C after 24 h of incubation with the molecules. Spots containing 5 μl, a 1:10 dilution, and a 1:100 dilution of cells are shown (left to right). (D) Growth on YPD plus 10% serum was performed as described for Fig. 1B. The percentage of hyphae is normalized to the percentage of hyphae formed when no molecule was added.

calf serum, Lee's medium, and M199 pH 8 tissue culture medium (Fig. 1B). Growth in Spider medium gave the most reproducible results, and thus this medium was used as the primary assay medium. These results indicated that this assay was amenable for the examination of alternative signals (media) that induce the budded-to-hyphal-form transition.

As a proof-of-concept experiment, the actin-depolymerizing drug latrunculin A and the known antifungal agent amphotericin B were tested in the assay. Addition of 1.6 μM latrunculin A inhibited the budded-to-hyphal-form transition and hyphal elongation at 37°C (Fig. 1C). This inhibition was dose dependent (the effect was lost at 0.1 μM) and reversible (data not shown). Similar dose-dependent inhibition was seen with amphotericin B (Fig. 1C). These results indicated that the assay was sensitive to known cytostatic and antifungal drugs and that the assay was amenable to dose dependency and reversibility studies.

Known and novel small molecules inhibited the budded-to-hyphal-form transition. With the assay, 72 molecules from a Chembridge small-molecule library were screened for inhibitory effects on the budded-to-hyphal-form transition. These molecules were initially identified in a screen for small molecules that inhibited the ability of the parasite *Toxoplasma gondii* to invade mammalian cells (10). Of the 72 molecules, 52 had no effect on budded growth or hyphal formation, 15 were either cytostatic or cytotoxic, leading to growth inhibition of budded cells, and 5 inhibited the budded-to-hyphal-form transition without affecting budded growth (Fig. 2A). Examination of the structures of the five bioactive molecules did not provide significant insight into their potential modes of action except that all five contained one or more hydrophobic groups that could allow the molecule to diffuse through the plasma membrane (see below).

The known actin-stabilizing drug jasplakinolide, which was added as a blinded control, was identified as one of the dose-dependent cytotoxic molecules that inhibited budded growth (Fig. 2B). Addition of 1 μM jasplakinolide led to cell cycle arrest with ≈85% small budded cells (Fig. 2B). Jasplakinolide

has been shown previously to have antifungal activity (37), and its identification in this screen further supported the efficacy of the assay in identifying inhibitors of budded growth.

The effects of the five bioactive molecules were also shown to be dose dependent and reversible (data not shown), and none inhibited budded growth for up to 24 h of incubation at 37°C (Fig. 2C). However, both amphotericin B and jasplakinolide exhibited dose-dependent cytotoxicity (Fig. 2C). These data indicated that the inhibition of the budded-to-hyphal-form transition by the bioactive molecules was not due to a cytostatic or cytotoxic effect.

Inhibition in this morphological assay (i.e., lack of hyphal cells) does not distinguish between inhibition of the budded-to-hyphal-form morphological transition and inhibition of hyphal elongation after the transition has taken place. To address this issue, SC5314 cells were induced in Spider medium for 2 h prior to the addition of the five bioactive molecules, and hyphal elongation was assayed 4 h after addition. All five molecules inhibited hyphal elongation (data not shown). Although the molecules were able to inhibit hyphal elongation, this result does not preclude potential effects on hyphal initiation as well.

The five bioactive molecules were also shown to have differential effects on other hypha-inducing media. All five molecules inhibited on Spider medium (Fig. 2A) and molecules 105249, 139598, 235236, and 152813 also inhibited on Lee's medium and M199 pH 8 medium (i.e., 0 to 6% hyphae relative to no-molecule addition; data not shown), but inhibition on YPD plus 10% fetal calf serum was less robust (29 to 54% hyphae relative to no-molecule addition; Fig. 2D). To test the potential synergy of these molecules, each pairwise combination of the molecules was examined in YPD plus 10% fetal calf serum. Whereas molecules 235236 and 121904 separately inhibited hyphal formation by ≈40%, addition of these molecules together inhibited hyphal formation by 100% (Fig. 2D) without affecting budded growth or cell viability. This effect was not seen with any other combinations of molecules (data not shown).

Bioactive molecules had differential effects on hypha-associated cellular processes. To further characterize the cellular phenotypes associated with addition of these bioactive molecules, hyphal form-specific gene expression in KTCa1 cells was assayed with the GFP reporter expressed under the control of the *HWP1* promoter (Fig. 3). *HWP1* transcriptional expression was strongly induced in response to hypha-inducing signals (38), including growth in Spider medium (Fig. 3A). Incubation of KTCa1 cells with the five bioactive molecules for 4 h at 37°C resulted in different levels of *HWP1 pr*-GFP expression, with 139598- and 121904-treated cells displaying higher levels of expression than 105249-, 152813-, and 235236-treated cells (Fig. 3A). It should be noted that the significant expression of *HWP1 pr*-GFP in 139598- and 121904-treated cells, which was comparable to *HWP1 pr*-GFP expression in hypha-inducing Spider medium, occurred in the absence of hyphal formation, reinforcing the notion that *HWP1* expression was not sufficient for hyphal formation and elongation (38).

Detectable *HWP1 pr*-GFP expression in budded cells treated with these molecules suggested that these molecules inhibited a protein or signaling pathway (i.e., the *CPH1*-dependent pathway) that either does not regulate *HWP1* expression (38) or functions downstream of *HWP1*. The low levels of *HWP1 pr*-GFP expression in cells treated with molecules 235236 and 105249 suggested that these molecules may inhibit a pathway (i.e., the *EFG1*-dependent pathway) leading to *HWP1* expression (38), which correlates well with the observation of rod-shaped *efg1*Δ-like cells in the 235236-treated population (Fig. 2A). The reason for the lack of rod-shaped *efg1*Δ-like cells in the 105249-treated population is unclear at this time.

The effects of the bioactive molecules on the assembly and maintenance of subcellular structures and organelles that have been associated with the induction of hyphal elongation, including septin rings, vacuoles, and the actin cytoskeleton (3, 15, 27, 29, 48), were examined. YAW2 cells expressing a septin Cdc10p-GFP fusion protein were used to examine septin organization. Addition of the molecules had no effect on the localization of the Cdc10p-GFP septin (data not shown), suggesting that the molecules did not disrupt septin organization.

As a measure of endocytosis and vacuolar function, the vital dye FM4-64 was added to treated cells. Cells grown in YNB and Spider medium produced budded and hyphal cells, respectively, that properly internalized FM4-64 into intracellular vacuoles (Fig. 3B). Internalization of FM4-64 into the vacuoles of hyphal cells took, on average, 2 h longer than it did in budded cells (data not shown). Normal endocytosis and vacuolar staining were observed in 152813-treated cells, but cells treated with 105249, 139598, 235236, and 121904 were unable to internalize the FM4-64, resulting in FM4-64's being trapped at the plasma membrane around the periphery of the cell. These results suggested that endocytosis was defective in these treated cells. As endocytosis depends on an intact actin cytoskeleton, a GFP-tagged actin-binding protein 1 (GFP-Abp1p) was used to examine the actin structures in the treated cells. Cells treated with 152813, 105249, 139598, 235236, and 121904 were able to polarize their actin cytoskeleton (data not shown), suggesting that the defects in endocytosis and hyphal formation were not the result of a depolarized actin cytoskeleton.

Structural derivatives of molecule 235236 had improved efficacy in inhibiting the budded-to-hyphal-form transition. To begin to characterize the potential functional groups of the bioactive molecules, structural derivatives of two molecules, 235236 and 139598, were examined for their inhibitory properties (Fig. 4). Molecule 235236 could inhibit the budded-to-hyphal-form transition at a 1 μM concentration, and two derivatives from the Chembridge library (molecules 5277651 and 5762974) could also inhibit at a 1 μM concentration (Fig. 4A). However, molecules 8003994 and 6022267 had reduced inhibitory properties and molecule 8003987 was not inhibitory. The 5277651 and 5762974 bioactive derivatives were further examined for their effects on different hypha-inducing media and subcellular structures. Both molecules were able to inhibit the budded-to-hyphal-form transition on YPD plus 10% serum to a much greater degree than the original molecule 235236 (Fig. 2D). As expected, the two derivatives were not cytotoxic (Fig. 2C) and affected HWP1-GFP expression and FM4-64 uptake similarly to molecule 235236 (data not shown).

The original bioactive molecule 139598 was effective at a 100 μM concentration, but none of its three structural derivatives tested were inhibitory at this concentration (Fig. 4B). It should

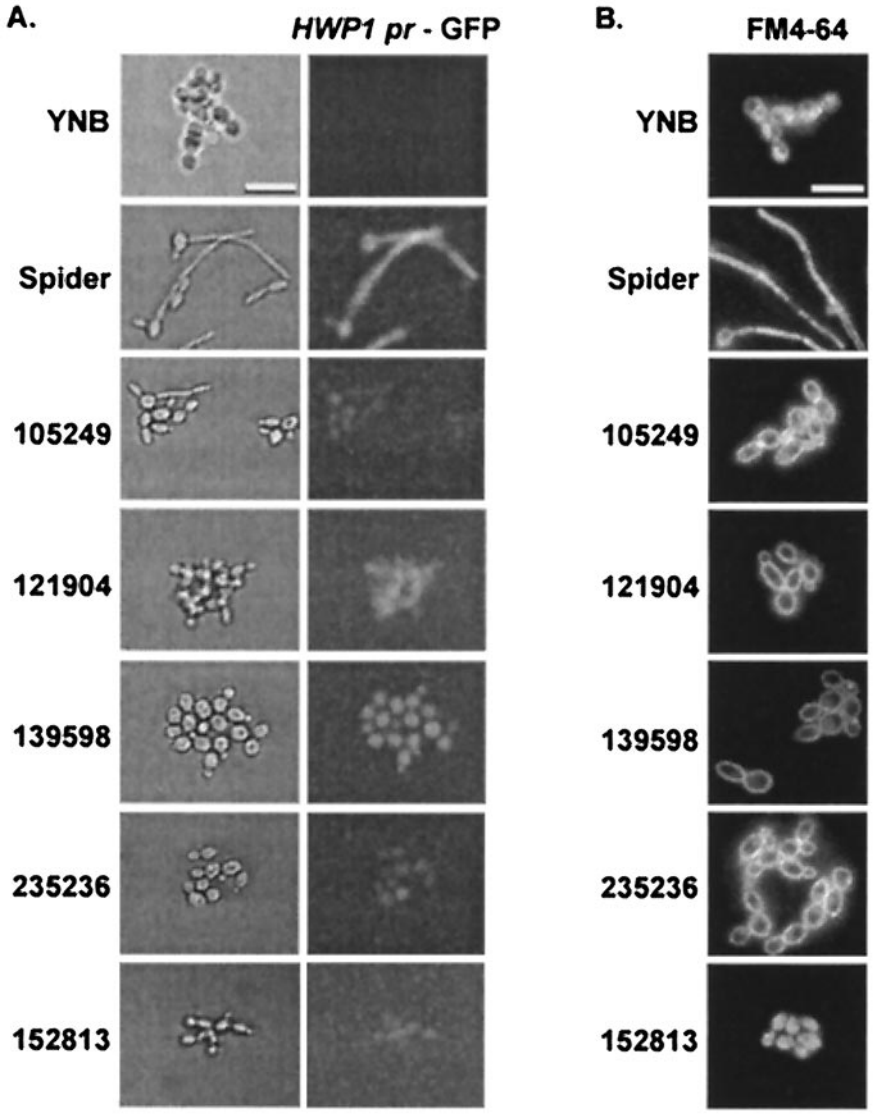

FIG. 3. Effects of small molecules on hyphal gene expression and endocytosis. (A) KTCa1 cells in Spider medium were added to 384-well microplates with an optical-glass bottom. Induction of *HWP1* expression was determined after 4 h of incubation. (B) To stain the vacuoles of SC5314 cells, the assay was carried out in optical-glass-bottomed microplates for 3 h, then FM4-64 was added, and the plate was returned to 37°C for 30 min. The medium containing FM4-64 was then aspirated out of each well, and 100 μl of fresh medium was added. The plate was returned to 37°C, and digital images of the cells were captured at 120 min with a 100× objective for wells containing budded cells or a 60× objective for wells containing hyphal cells.

be noted that any conclusions or predictions from these limited structural studies would be premature and must await more detailed examination of different structural variants.

Molecules 152813 and 5762974 protected endothelial cells from *C. albicans*-dependent damage. An in vitro endothelial cell damage assay was used to determine whether the small molecules could protect endothelial cells from damage by *C. albicans* (32). All of the molecules induced release of ^{51}Cr at concentrations of 1 μM, and this ability was dose dependent, indicating that the tested molecules had some toxic effect on endothelial cells (Fig. 5A and data not shown). However, when the small molecules were assayed with *C. albicans* cells, two of the small molecules, 152813 and 5762974, were able to reduce *C. albicans*-dependent ^{51}Cr release in a dose-dependent manner (Fig. 5B). In fact, at a concentration of 100 μM, molecule 5762974 almost completely eliminated *C. albicans*-induced endothelial injury. This reduction in endothelial injury was likely due to prevention of hyphal formation, since *C. albicans* cells incubated on endothelial cells in the presence of these two molecules remained predominantly in the budded form, as determined by microscopic examination (data not shown). In contrast, molecules 105249 and 121904 did not inhibit hyphal formation at a concentration of 400 μM in the presence of endothelial cells (data not shown), so they were not included in these assays. Of the three related molecules (235236, 527751, and 5762974), only 5762974 was included in these assays.

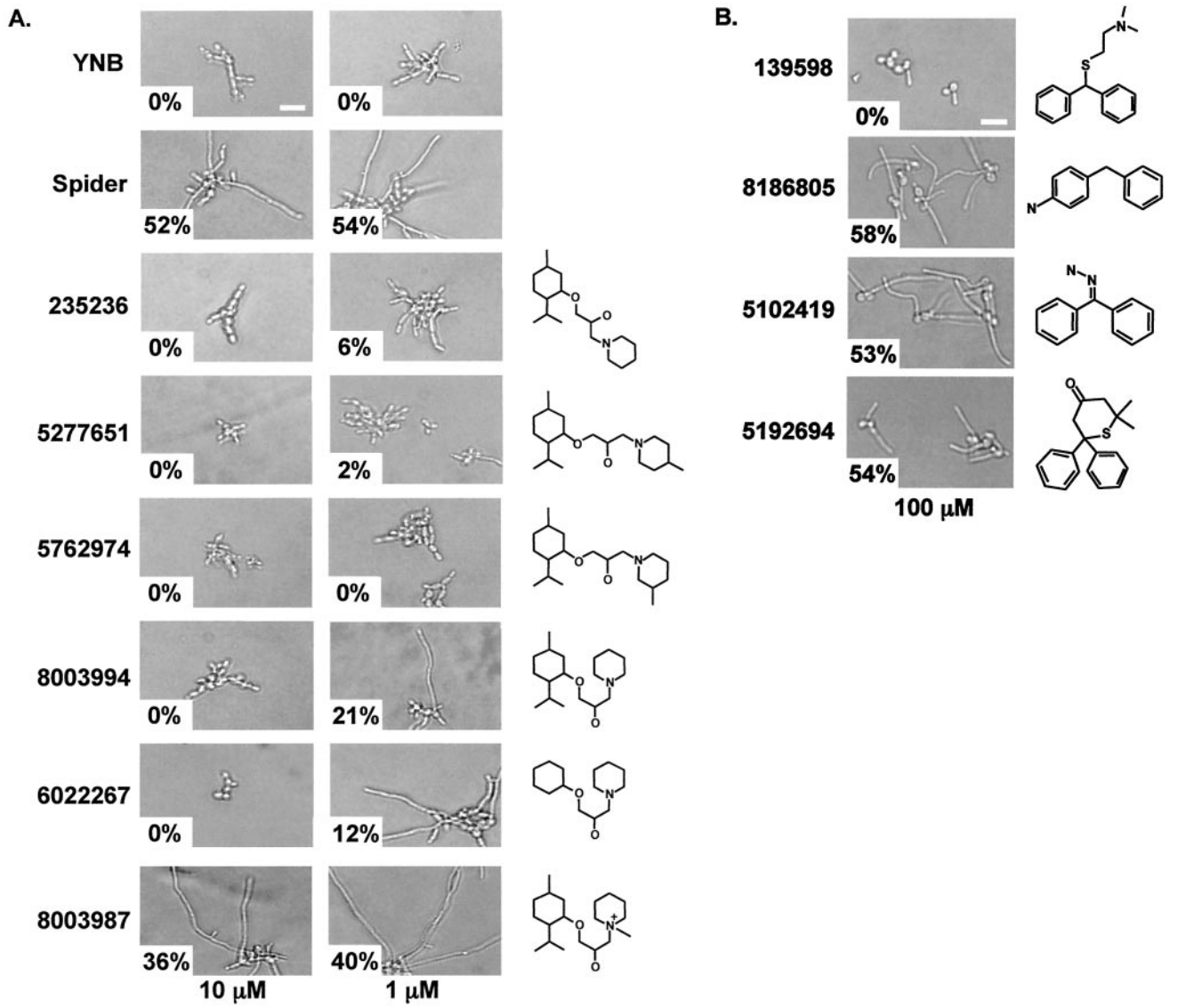

FIG. 4. Effects of structural variants of molecules 235236 and 139598. (A) The Chembridge catalog number and chemical structures of structural variants of molecule 235236 are shown. Molecules were tested at 10 and 1 μM concentrations with the assay described for Fig. 1B. The percentage of hyphae observed is shown in the lower left of each photomicrograph. (B) The Chembridge catalog number and chemical structures of structural variants of molecule 139598 are shown. Molecules were tested at 100 μM concentrations with the assay described for Fig. 1B. The percentage of hyphae observed is shown in the lower left of each photomicrograph.

DISCUSSION

Current antifungal therapies are limited to drugs that inhibit the growth of *C. albicans* cells rather than specific virulence processes. Unfortunately, these drugs, such as amphotericins, azoles, and echinocandins, also have inhibitory effects on the growth and viability of host cells, leading to serious side effects for the host. This new approach to discovering possible antifungal therapeutics described herein is based on the ability of small organic molecules to inhibit the budded-to-hyphal-form transition without affecting the growth of *C. albicans* cells. Data from a number of laboratories have indicated that the budded-to-hyphal-form transition is required for *C. albicans* virulence (12, 16, 19–21, 33, 40, 52). Since these small molecules do not inhibit normal mitotic growth, it is likely that essential proteins and processes needed for polarized growth and cell cycle progression are not being affected. Research is under way to examine the potential effects of the compounds on mammalian cells and on the virulence of treated *C. albicans* cells in a mouse model of disseminated candidiasis.

Using a microtiter plate-based morphological assay that can be adapted for high throughput, we have identified five novel molecules that inhibit the budded-to-hyphal-form transition and hyphal growth without affecting budded cell growth. These molecules were identified from a selected collection of 72 molecules, some of which had previously been shown to inhibit *Toxoplasma gondii* invasion of mammalian cells (10). Therefore, this high percentage of hits (5 of 72) is probably not

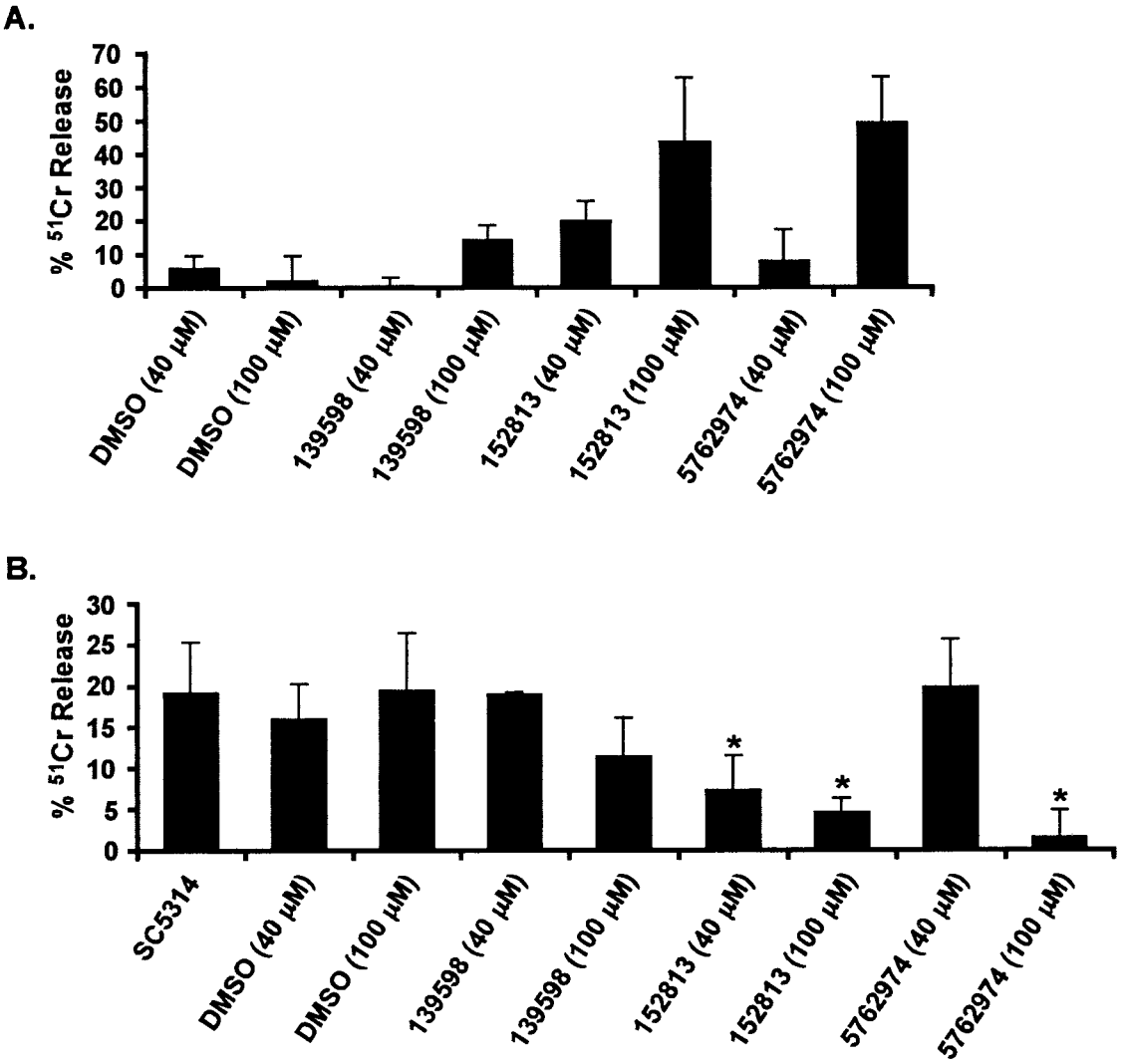

FIG. 5. Effects of small molecules on ^{51}Cr release from endothelial cells. (A) Endothelial cells were incubated with the small molecules in dimethyl sulfoxide at the indicated concentrations in the absence of *C. albicans* cells (toxicity studies). Results are the averages of three experiments, with the amount of spontaneous ^{51}Cr released in the absence of added molecules subtracted after adding an equal amount of the diluent dimethyl sulfoxide. (B) Endothelial cells were incubated with the indicated small molecules and cocultured with *C. albicans* cells. Results are the averages of three experiments, with the amount of ^{51}Cr released in part A subtracted. Asterisks indicate a P value of < 0.004 compared to cells treated with dimethyl sulfoxide, as determined by the Wilcoxon rank sum test.

indicative of the number of random small molecules that will be able to inhibit the budded-to-hyphal-form transition.

Attempts to group these bioactive molecules based on their chemical structures was not productive, as structural similarities between the molecules were limited to hydrophobic groups most likely required for passage through the plasma membrane. Attempts to find commonalities among the molecules based on their cellular effects were more fruitful. One molecule, 152813, had low levels of transcriptional induction of the hyphal form-specific *HWP1* promoter without being affected in endocytosis, while molecules 121904 and 139598 inhibited endocytosis without affecting promoter induction. A third subset consisting of molecules 105249 and 235236 inhibited both hyphal form-specific promoter induction and endocytosis. These differential effects raise the possibility that the small molecules are inhibiting specific signaling pathways that lead to multiple cellular outputs as opposed to proteins involved in the mechanics of these processes. In addition, the synergistic effects of molecules 235236 and 121904 suggest that these molecules are acting on separate signaling pathways. Other interpretations of these synergistic effects are certainly possible, and testing of these hypotheses will necessitate the identification of the cellular targets for these small molecules.

The hyphal form-specific cell wall protein Hwp1p is involved in the adhesion of *C. albicans* cells to human epithelium (44). Its transcription is regulated by the Efg1p transcription factor in response to hypha-inducing signals transduced via the Pka1p-dependent signal transduction pathway (5). The inhibition of the hyphal form-specific induction of the *HWP1* promoter by molecules 152813, 105249, and 235236 suggests that these molecules block the signaling cascades that lead to Efg1p-dependent gene induction. The rod-shaped *efg1*Δ-like

morphology of cells treated with molecule 235236 further supports the possibility that molecule 235236 is negatively impinging upon the Efg1p-dependent signaling cascades. This inhibition is either from a direct impact on one of the proteins involved in signaling or an indirect effect on another cellular pathway that impinges on these signaling pathways. Experiments are under way to determine the specific signaling pathways affected by each molecule.

The role of endocytosis in the budded-to-hyphal-form transition and/or hyphal growth is not well understood. Mutations in *C. albicans* Sla2p, which is involved in both organization of the actin cytoskeleton and endocytosis, are defective in the formation of hyphae (2), suggesting a possible role for endocytosis in hyphal formation and/or elongation. The actin cytoskeleton in cells treated with these small molecules was properly polarized, suggesting that the endocytosis defect observed with cells treated with molecules 121904, 139598, 105249, and 235236 may be independent of the actin cytoskeleton. Interestingly, molecules 105249 and 235236 blocked both the induction of a hyphal form-specific gene and endocytosis, suggesting that there may be a link between the signaling cascades involved in the budded-to-hyphal-form transition and the regulation of endocytosis. This result may also explain why the small molecules block both the budded-to-hyphal-form transition and hyphal elongation; continued signaling via hyphal form-specific signal transduction cascades may be required to maintain hyphal elongation through cellular processes such as endocytosis.

Deletion mutations that inhibit the budded-to-hyphal-form transition have previously been shown to lead to a decrease in *C. albicans* virulence. Therefore, small-molecule inhibitors that block either the budded-to-hyphal-form transition or hyphal growth should also attenuate virulence. Two of the small-molecule inhibitors were able to inhibit *C. albicans*-dependent endothelial cell injury. This result suggests that blocking the budded-to-hyphal-form transition and/or hyphal growth through the addition of bioactive molecules is likely to reduce the virulence of *C. albicans* cells; a recent study by Sanchez et al. demonstrated a relationship between *C. albicans* virulence during experimental hematogenously disseminated infection and endothelial cell damage in vitro (35). However, the ability of these small molecules to cause ^{51}Cr release from endothelial cells on their own must first be minimized through further analysis of new structural derivatives.

The experiments described herein lay the foundation for providing a new antifungal therapeutic paradigm in which small molecules inhibit an essential virulence process (budded-to-hyphal-form transition) instead of cell growth in *C. albicans.* Studies to validate this paradigm with an animal model of hematogenously disseminated candidiasis are under way.

ACKNOWLEDGMENTS

We thank Gary Ward, Kim Carey, James Konopka, Peter Sudbery, Aaron Mitchell, and Paula Sundstrom for valuable reagents and Gary Ward, Kim Carey, Tammy Richman, Dana Davis, Judy Berman, and members of the Johnson laboratory for valuable discussions and critical comments on the manuscript.

This research was supported by a J. Walter Juckett Scholar Award to D.I.J. from the Lake Champlain Cancer Research Organization and the Vermont Cancer Center and by Public Health Service grants RO1AI-19990 and PO1AI-37194 awarded to J.E.E.

REFERENCES

1. **Akashi, T., T. Kanbe, and K. Tanaka.** 1994. The role of the cytoskeleton in the polarized growth of the germ tube in *Candida albicans*. Microbiology **140:**271–280.
2. **Asleson, C. M., E. S. Bensen, C. A. Gale, A. S. Melms, C. Kurischko, and J. Berman.** 2001. *Candida albicans INT1*-induced filamentation in *Saccharomyces cerevisiae* depends on Sla2p. Mol. Cell. Biol. **21:**1272–1284.
3. **Bahn, Y. S., and P. Sundstrom.** 2001. *CAP1*, an adenylate cyclase-associated protein gene, regulates bud-hypha transitions, filamentous growth, and cyclic AMP levels and is required for virulence of *Candida albicans*. J. Bacteriol. **183:**3211–3223.
4. **Birse, C. E., M. Y. Irwin, W. A. Fonzi, and P. S. Sypherd.** 1993. Cloning and characterization of *ECE1*, a gene expressed in association with cell elongation of the dimorphic pathogen *Candida albicans*. Infect. Immun. **61:**3648–3655.
5. **Braun, B. R., and A. D. Johnson.** 2000. *TUP1*, *CPH1* and *EFG1* make independent contributions to filamentation in *Candida albicans*. Genetics **155:**57–67.
6. **Brown, A. J. P.** 2002. Expression of growth form-specific factors during morphogenesis in *Candida albicans*, p. 87–93. *In* R. A. Calderone (ed.), *Candida* and candidiasis. ASM Press, Washington, D.C.
7. **Brown, A. J. P.** 2002. Morphogenetic signaling pathways in *Candida albicans*, p. 95–106. *In* R. A. Calderone (ed.), *Candida* and candidiasis. ASM Press, Washington, D.C.
8. **Brown, A. J. P., and N. A. R. Gow.** 1999. Regulatory networks controlling *Candida albicans* morphogenesis. Trends Microbiol. **7:**333–338.
9. **Buffo, J., M. A. Herman, and D. R. Soll.** 1984. A characterization of pH-regulated dimorphism in *Candida albicans*. Mycopathologia **85:**21–30.
10. **Carey, K. L., N. J. Westwood, T. J. Mitchison, and G. E. Ward.** 2004. A small-molecule approach to studying invasive mechanisms of *Toxoplasma gondii*. Proc. Natl. Acad. Sci. USA **101:**7433–7438.
11. **Crews, C. M., and U. Splittgerber.** 1999. Chemical genetics: exploring and controlling cellular processes with chemical probes. Trends Biochem. Sci. **24:**317–320.
12. **Csank, C., K. Schröppel, E. Leberer, D. Harcus, O. Mohamed, S. Meloche, D. Y. Thomas, and M. Whiteway.** 1998. Roles of the *Candida albicans* mitogen-activated protein kinase homolog, Cek1p, in hyphal development and systemic candidiasis. Infect. Immun. **66:**2713–2721.
13. **Edmond, M. B., S. E. Wallace, D. K. McClish, M. A. Pfaller, R. N. Jones, and R. P. Wenzel.** 1999. Nosocomial bloodstream infections in United States hospitals: a three-year analysis. Clin. Infect. Dis. **29:**239–244.
14. **Feng, Q. H., E. Summers, B. Guo, and G. Fink.** 1999. Ras signaling is required for serum-induced hyphal differentiation in *Candida albicans*. J. Bacteriol. **181:**6339–6346.
15. **Hazan, I., and H. Liu.** 2002. Hyphal tip-associated localization of Cdc42 is F-actin dependent in *Candida albicans*. Eukaryot. Cell **1:**856–864.
16. **Hube, B., D. Hess, C. A. Baker, M. Schaller, W. Schafer, and J. W. Dolan.** 2001. The role and relevance of phospholipase D1 during growth and dimorphism of *Candida albicans*. Microbiology **147:**879–889.
17. **Köhler, J. R., and G. R. Fink.** 1996. *Candida albicans* strains heterozygous and homozygous for mutations in mitogen-activated protein kinase signaling components have defects in hyphal development. Proc. Natl. Acad. Sci. USA **93:**13223–13228.
18. **Kurtz, M. B., M. W. Cortelyou, and D. R. Kirsch.** 1986. Integrative transformation of *Candida albicans*, using a cloned Candida *ADE2* gene. Mol. Cell. Biol. **6:**142–149.
19. **Leberer, E., D. Harcus, I. D. Broadbent, K. L. Clark, D. Dignard, K. Ziegelbauer, A. Schmidt, N. A. R. Gow, A. J. P. Brown, and D. Y. Thomas.** 1996. Signal transduction through homologs of the Ste20p and Ste7p protein kinases can trigger hyphal formation in the pathogenic fungus *Candida albicans*. Proc. Natl. Acad. Sci. USA **93:**13217–13222.
20. **Leberer, E., D. Harcus, D. Dignard, L. Johnson, S. Ushinsky, D. Y. Thomas, and K. Schroppel.** 2001. Ras links cellular morphogenesis to virulence by regulation of the MAP kinase and cAMP signalling pathways in the pathogenic fungus *Candida albicans*. Mol. Microbiol. **42:**673–687.
21. **Leberer, E., K. Ziegelbauer, A. Schmidt, D. Harcus, D. Dignard, J. Ash, L. Johnson, and D. Y. Thomas.** 1997. Virulence and hyphal formation of *Candida albicans* require the Ste20p-like protein kinase CaCla4p. Curr. Biol. **7:**539–546.
22. **Lee, K. L., H. R. Buckley, and C. C. Campbell.** 1975. An amino acid liquid synthetic medium for the development of mycelial and yeast forms of *Candida albicans*. Sabouraudia **13:**148–153.
23. **Lengeler, K. B., R. C. Davidson, C. D'Souza, T. Harashima, W. C. Shen, P. Wang, X. W. Pan, M. Waugh, and J. Heitman.** 2000. Signal transduction cascades regulating fungal development and virulence. Microbiol. Mol. Biol. Rev. **64:**746–785.
24. **Liu, H., J. Köhler, and G. R. Fink.** 1994. Suppression of hyphal formation in *Candida albicans* by mutation of a *STE12* homolog. Science **266:**1723–1726.
25. **Lo, H. J., J. R. Kohler, B. DiDomenico, D. Loebenberg, A. Cacciapuoti, and G. R. Fink.** 1997. Nonfilamentous *C. albicans* mutants are avirulent. Cell **90:**939–949.

26. **Mitchell, A. P.** 1998. Dimorphism and virulence in *Candida albicans*. Curr. Opin. Microbiol. **1:**687–692.
27. **Oberholzer, U., A. Marcil, E. Leberer, D. Y. Thomas, and M. Whiteway.** 2002. Myosin I is required for hypha formation in *Candida albicans*. Eukaryot. Cell **1:**213–228.
28. **Odds, F. C.** 1994. Pathogenesis of Candida infections. J. Am. Acad. Dermatol. **31:**S2–S5.
29. **Palmer, G. E., A. Cashmore, and J. Sturtevant.** 2003. *Candida albicans VPS11* is required for vacuole biogenesis and germ tube formation. Eukaryot. Cell. **2:**411–421.
30. **Perea, S., and T. F. Patterson.** 2002. Antifungal resistance in pathogenic fungi. Clin. Infect. Dis. **35:**1073–1080.
31. **Peterson, J. R., and T. J. Mitchison.** 2002. Small molecules, big impact: a history of chemical inhibitors and the cytoskeleton. Chem. Biol. **9:**1275–1285.
32. **Phan, Q. T., P. H. Belanger, and S. G. Filler.** 2000. Role of hyphal formation in interactions of *Candida albicans* with endothelial cells. Infect. Immun. **68:**3485–3490.
33. **Richard, M., S. Ibata-Ombetta, F. Dromer, F. Bordon-Pallier, T. Jouault, and C. Gaillardin.** 2002. Complete glycosylphosphatidylinositol anchors are required in *Candida albicans* for full morphogenesis, virulence and resistance to macrophages. Mol. Microbiol. **44:**841–853.
34. **Sambrook, J., E. F. Fritsch, and T. Maniatis.** 1989. Molecular cloning: a laboratory manual, 2nd ed. Cold Spring Harbor Laboratory Press, Cold Spring Harbor, N.Y.
35. **Sanchez, A. A., D. A. Johnston, C. Myers, J. J. E. Edwards, A. P. Mitchell, and S. G. Filler.** 2004. Relationship between *Candida albicans* virulence during experimental hematogenously disseminated infection and endothelial cell damage in vitro. Infect. Immun. **72:**598–601.
36. **Schmidt-Westhausen, A., R. A. Schiller, H. D. Pohle, and P. A. Reichart.** 1991. Oral Candida and Enterobacteriaceae in HIV-1 infection: correlation with clinical candidiasis and antimycotic therapy. J. Oral Pathol. Med. **20:** 467–472.
37. **Scott, V. R., R. Boehme, and T. R. Matthews.** 1988. New class of antifungal agents: jasplakinolide, a cyclodepsipeptide from the marine sponge, *Jaspis* species. Antimicrob. Agents Chemother. **32:**1154–1157.
38. **Sharkey, L. L., M. D. McNemar, S. M. Saporito-Irwin, P. S. Sypherd, and W. A. Fonzi.** 1999. *HWP1* functions in the morphological development of *Candida albicans* downstream of *EFG1*, *TUP1*, and *RBF1*. J. Bacteriol. **181:** 5273–5279.
39. **Sherman, F., G. R. Fink, and J. B. Hicks.** 1986. Methods in yeast genetics: a laboratory manual. Cold Spring Harbor Laboratory Press, Cold Spring Harbor, N.Y.
40. **Singh, P., S. Ghosh, and A. Datta.** 2001. Attenuation of virulence and changes in morphology in *Candida albicans* by disruption of the *N*-acetylglucosamine catabolic pathway. Infect. Immun. **69:**7898–7903.
41. **Sonneborn, A., D. P. Bockmuhl, M. Gerads, K. Kurpanek, D. Sanglard, and J. F. Ernst.** 2000. Protein kinase A encoded by *TPK2* regulates dimorphism of *Candida albicans*. Mol. Microbiol. **35:**386–396.
42. **Staab, J. F., Y.-S. Bahn, and P. Sundstrom.** 2003. Integrative, multifunctional plasmids for hypha-specific or constitutive expression of green fluorescent protein in *Candida albicans*. Microbiology **149:**2977–2986.
43. **Stoldt, V. R., A. Sonneborn, C. E. Leuker, and J. F. Ernst.** 1997. Efg1p, an essential regulator of morphogenesis of the human pathogen *Candida albicans*, is a member of a conserved class of bHLH proteins regulating morphogenetic processes in fungi. EMBO J. **16:**1982–1991.
44. **Sundstrom, P., E. Balish, and C. M. Allen.** 2002. Essential role of the *Candida albicans* transglutaminase substrate, hyphal wall protein 1, in lethal oroesophageal candidiasis in immunodeficient mice. J. Infect. Dis. **185:**521–530.
45. **Tsukahara, K., K. Hata, K. Nakamoto, K. Sagane, N. Watanabe, J. Kuromitsu, J. Kai, M. Tsuchiya, F. Ohba, Y. Jigami, K. Yoshimatsu, and T. Nagasu.** 2003. Medicinal genetics approach towards identifying the molecular target of a novel inhibitor of fungal cell wall assembly. Mol. Microbiol. **48:**1029–1042.
46. **vandenBerg, A. L., A. S. Ibrahim, J. E. Edwards, Jr., K. A. Toenjes, and D. I. Johnson.** 2004. Cdc42p GTPase regulates the budded-to-hyphal-form transition and the expression of hypha-specific transcripts in *Candida albicans*. Eukaryot. Cell **3:**724–734.
47. **Ward, G. E., K. L. Carey, and N. J. Westwood.** 2002. Using small molecules to study big questions in cellular microbiology. Cell. Microbiol. **4:**471–482.
48. **Warenda, A. J., S. Kauffman, T. P. Sherrill, J. A. Becker, and J. B. Konopka.** 2003. *Candida albicans* septin mutants are defective for invasive growth and virulence. Infect. Immun. **71:**4045–4051.
49. **Warenda, A. J., and J. B. Konopka.** 2002. Septin function in *Candida albicans* morphogenesis. Mol. Biol. Cell **13:**2732–2746.
50. **White, T. C., K. A. Marr, and R. A. Bowden.** 1998. Clinical, cellular, and molecular factors that contribute to antifungal drug resistance. Clin. Microbiol. Rev. **11:**382–402.
51. **Wilson, R. B., D. Davis, and A. P. Mitchell.** 1999. Rapid hypothesis testing with *Candida albicans* through gene disruption with short homology regions. J. Bacteriol. **181:**1868–1874.
52. **Yaar, L., M. Mevarech, and Y. Koltin.** 1997. A *Candida albicans* RAS-related gene (*CaRSR1*) is involved in budding, cell morphogenesis and hypha development. Microbiol. UK **143:**3033–3044.
53. **Yokoyama, K., H. Kaji, K. Nishimura, and M. Miyaji.** 1994. The role of microfilaments and microtubules during pH-regulated morphological transition in *Candida albicans*. Microbiology **140:**281–287.